THE JOURNAL OF PHYSICAL CHEMISTRY Letters

Letter

pubs.acs.org/JPCL

# Amide Rotation Hindrance Predicts Proteolytic Resistance of Cystine-Knot Peptides

Yanzi Zhou,*[,†] Daiqian Xie,[†] and Yingkai Zhang*[,‡,§]

[†]Laboratory of Mesoscopic Chemistry, Collaborative Innovation Center of Chemistry for Life Sciences, Institute of Theoretical and Computational Chemistry, School of Chemistry and Chemical Engineering, Nanjing University, Nanjing 210023, China

[‡]Department of Chemistry, New York University, New York, New York 10003 United States

[§]NYU-ECNU Center for Computational Chemistry at NYU Shanghai, Shanghai 200062, China

Supporting Information

**ABSTRACT:** Cystine-knot peptides have remarkable stability against protease degradation and are attractive scaffolds for peptide-based therapeutic and diagnostic agents. In this work, by studying the hydrolysis reaction of a cystine-knot inhibitor MCTI-A and its variants with ab initio QM/MM molecular dynamics simulations, we have elucidated an amide rotation hindrance mechanism for proteolysis resistance: The proteolysis of MCTI-A is retarded due to the higher free energy cost during the rotation of NH group around scissile peptide bond at the tetrahedral intermediate of acylation, and covalent constraint provided by disulfide bonds is the key factor to hinder this rotation. A nearly linear correlation has been revealed between free energy barriers of the peptide hydrolysis reaction and the amide rotation free energy changes at the protease–peptide Michaelis complex state. This suggests that amide rotation hindrance could be one useful feature to estimate peptide proteolysis stability.

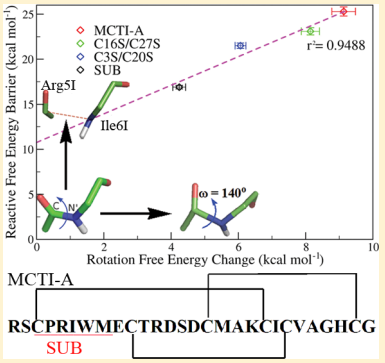


Cystine-knot peptides, also known as knottins and characterized by at least three disulfide bonds, have emerged as promising candidates for the development of peptide-based therapeutic and diagnostic agents.[1−5] Different from some other classes of peptide molecules, one of the most attractive feature of cystine-knot peptides is their remarkable proteolytic resistance. In fact, some cystine-knot peptides, such as BPTI and MCTI-A,[6−8] are known to be very potent canonical serine proteinases inhibitors, which bind to the enzyme active site in a substrate manner but can resist proteolysis ranging from hours to even years.[9−12] This poses a classic puzzle that confronts fundamental principle of enzyme specificity.

Two main mechanistic hypotheses have been put forward to explain canonical serine proteinases inhibitors' surprising lack of reactivity: one is the Laskowski mechanism,[11−13] and the other is clogged mechanism.[14−16] Although both mechanisms have tried to account for the effect of conformational constraints on the proteolytic resistance, no direct evidence has been provided, and there is no quantitative relationship revealed between geometry factors and the slow-down of kinetic hydrolytic rate.[6,7] In this work, by employing Born–Oppenheimer ab initio QM/MM molecular dynamics simulations[17,18] and umbrella sampling,[19,20] a state-of-the-art approach to simulate biological reactions, we have discovered a novel amide rotation hindrance mechanism regarding how disulfide constraint leads to proteolysis resistance. Furthermore, we have uncovered a nearly linear correlation between free energy barriers of the peptide hydrolysis reaction and the amide rotation free energy changes at the Michaelis complex (EI state).

Our study initially focuses on a cystine-knot peptide MCTI-A, a potent trypsin inhibitor of the squash family with 28 amino acid residues. The scheme of its cystine-knot motif with disulfide bonding pattern is presented in Figure 1, in which the first three cysteine residues (C3, C10, C16) form disulfide bonds with the last three cysteine (C20, C22, C27) in a consecutive manner, respectively, and the red ribbon indicates the peptide ring of MCTI-A connected by Cys3-Cys20 and Cys10-Cys22 disulfide bridges. In the high-resolution crystal structure of the binding complex formed by porcine $\beta$-trypsin with the MCTI-A inhibitor (PDB ID: 1MCT),[8] as shown in Figure S2, it interacts with trypsin active site like the corresponding hexapeptide substrate Cys3-Pro4-Arg5-Ile6-Trp7-Met8. Previously, we have studied the acylation reaction of the scissile bond between Arg5-Ile6 for the same trypsin–hexapeptide complex[21] by employing B3LYP/6-31+G* QM/MM MD simulations[17,18] with the pseudobond approach.[22−24] The calculated overall free energy barrier of 16.9 kcal/mol indicates that this hexapeptide can be easily acylated by porcine $\beta$-trypsin, consistent with other theoretical studies that this is a substrate.[25,26] This sets the stage for us to probe how the cystine-knot peptide can resist proteolysis.

**Received:** February 18, 2016
**Accepted:** March 9, 2016
**Published:** March 9, 2016






DOI: 10.1021/acs.jpclett.6b00373
J. Phys. Chem. Lett. 2016, 7, 1138−1142

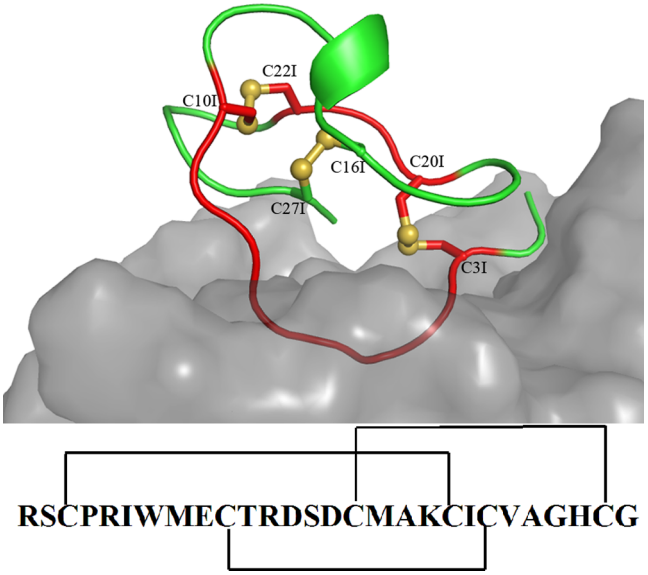


**Figure 1.** Illustration of the cystine-knot structure for MCTI-A complexed with trypsin. MCTI-A is shown in cartoon mode, while trypsin is in surface mode. The red ribbon indicates that two pairs of disulfide bridges (3−20 and 10−22) form an amino acid residue ring.

The first task is to employ the same simulation protocol to computationally characterize the corresponding acylation reaction of full-length cystine-knot peptide MCTI-A catalyzed by porcine $\beta$-trypsin. The detailed computational protocol is presented in the Supporting Information. Our computational results (Figure 2 and Table S1) indicate that the acylation

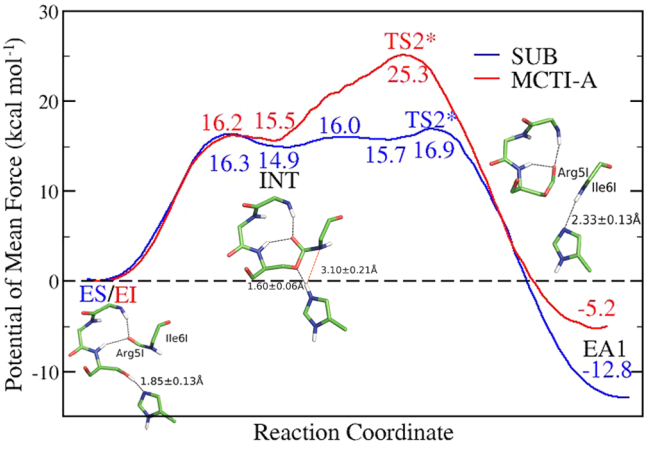


**Figure 2.** Free energy profile for acylation reaction of the trypsin-catalyzed MCTI-A and SUB hydrolysis. The structures for MCTI-A−trypsin at the reactant, intermediate, and product states are also illustrated.

reaction of MCTI-A hydrolyzed by trypsin shares a similar catalytic mechanism as the hexapeptide substrate (SUB)[21] but has a significantly high reaction barrier of 25.3 kcal/mol in comparison with 16.9 kcal/mol for the hexapeptide. The acylation reaction of MCTI-A would be about one million times slower than SUB, which is consistent with experimental results that MCTI-A is a potent inhibitor of porcine $\beta$-trypsin and its strong resistance to hydrolysis mainly comes from the acylation stage. Interestingly, as shown in Figure 2, MCTI-A and SUB have almost the same free energy barrier (16.2 vs 16.3 kcal/mol) for the initial nucleophilic attack step, in which His57 acts as a general base accepting a proton from Ser195, and the OG atom of Ser195 attacks the carbonyl carbon atom of substrate Arg5 to form a metastable tetrahedral intermediate INT. Thus, our simulation results do not support one explanation of Laskowski mechanism that the proteolysis resistance comes from the failure to form the reactive nucleophilic attack complex at the reactant state of the acylation stage.[27,28] Meanwhile, although the leaving of C-terminal product fragment is hindered by the 3−20 disulfide and the $NH_2$ group of cleaved MCTI-A is in excellent position to reattack the acyl C═O (see Figure 2, EA1 state), the free energy barrier for the reverse reaction is 5.2 kcal/mol higher than the forward one. Thus, our study does not support the clogged mechanism either, in which the reverse reaction of the acylation is suggested to more rapidly occur to reform the peptide bond.[14−16]

Figure 2 clearly indicates that the main difference between MCTI-A and SUB comes from the free energy change between INT and TS2*: It is 9.8 kcal/mol for the MCTI-A, while it is only 2.0 kcal/mol for the substrate. From INT to TS2*, the main atomic motions involve both a subtle reorientation of the His57 ring and the rotation of the leaving group around the scissile C−N bond, which is defined as $\omega$ angle in Figure 3. It

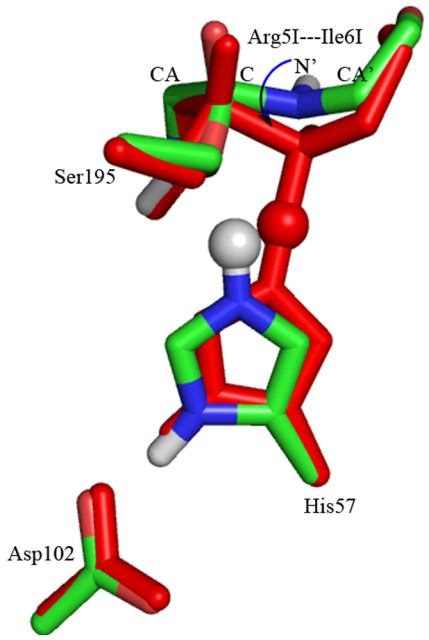


**Figure 3.** Deviation of active site at TS2* state from INT state along the reaction path. INT state is colored by element, and TS2* state is colored red. The whole structure is shown in stick mode, except that the transferring H atom is shown in sphere. Torsion angle $\omega$: CA−C−N′−CA′ is defined to monitor the rotation of the scissile peptide bond.

should be noted that reorientation of the His57 ring only involves the enzyme, which is the same between MCTI-A and the SUB. Meanwhile, from Table 1, we can see that torsion angle $\omega$ of the scissile C−N bond adopts a very similar value of ∼140° at TS2*, while it is quite different at INT (∼170° for MCTI-A versus ∼160° for SUB). Even at the reactant state, we can see that the torsion angle $\omega$ of the scissile C−N bond, which would favor the planar due to its $sp^2$ character, is easier to be deviated from 180° in the SUB than in the MCTI-A.



DOI: 10.1021/acs.jpclett.6b00373
J. Phys. Chem. Lett. 2016, 7, 1138−1142

**Table 1. Change of Torsion Angle $\omega$/Degree during Acylation Reaction for Inhibitors and Substrate Based on B3LYP/6-31+G* QM/MM MD Simulations**

| $\omega$/degree | EI/ES | TS1 | INT | TS2* |
|---|---|---|---|---|
| wild type | 178.8 ± 7.9 | 174.1 ± 7.6 | 170.7 ± 7.6 | 140.4 ± 5.4 |
| C3S/C20S | 177.1 ± 6.9 | 174.1 ± 7.3 | 170.0 ± 6.3 | 141.0 ± 6.4 |
| C16S/C27S | 178.2 ± 7.2 | 174.4 ± 6.3 | 169.2 ± 6.5 | 139.8 ± 5.3 |
| SUB | 173.5 ± 8.3 | 162.9 ± 7.4 | 160.5 ± 8.3 | 140.0 ± 5.5 |

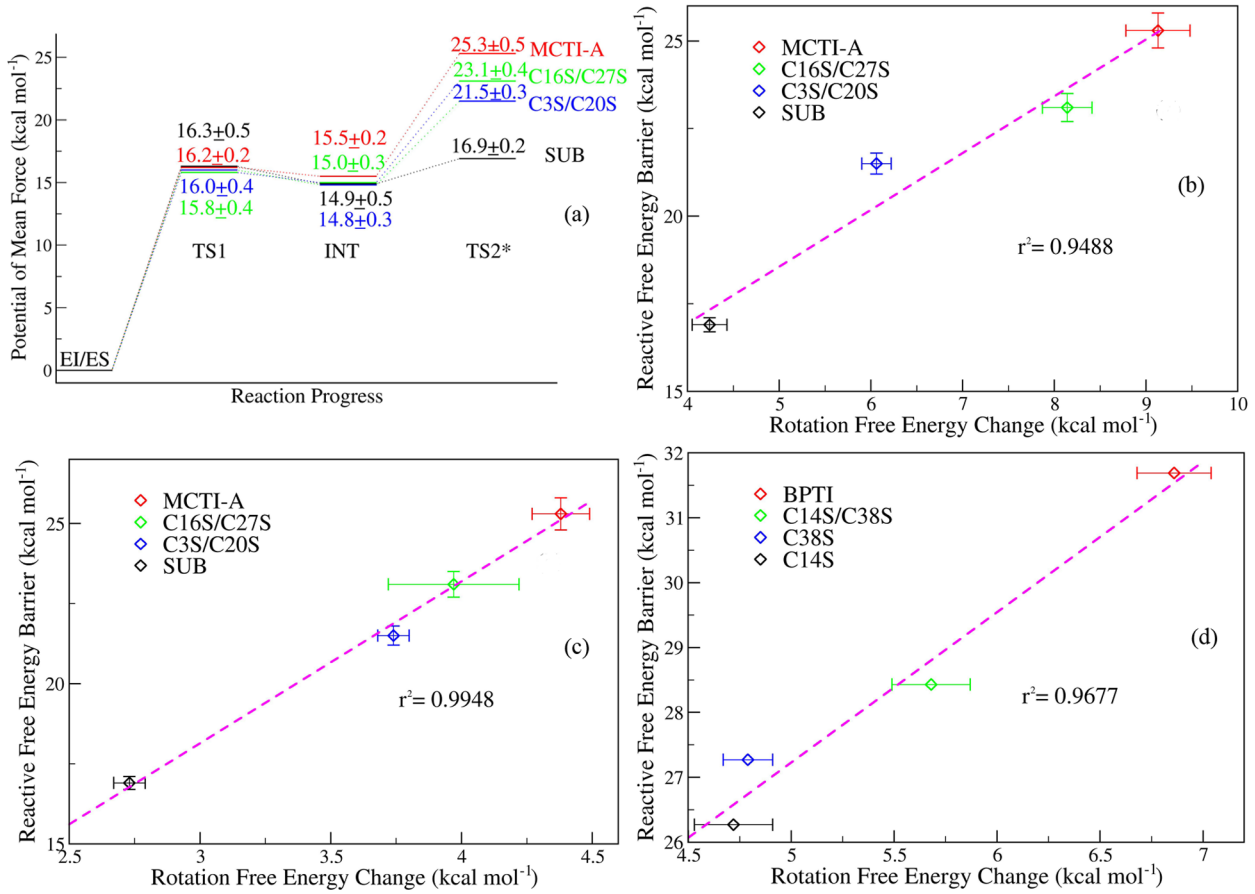


**Figure 4.** (a) Free energy profiles of acylation reaction for trypsin−SUB and trypsin−inhibitors. (b,c) Correlation between the free energy for the torsion angle $\omega$ rotating to 140° at the reaction complexes and the free energy barrier in acylation step for trypsin−SUB and trypsin−inhibitors. (b) Rotation free energy changes are calculated from QM/MM-MD simulations. (c) Rotation free energy changes are from classical MD simulations. (d) Correlation between the free energy for the torsion angle $\omega$ rotating to 140° at the reaction complexes from classic MD simulations and the experimental reactive free energy barrier for trypsin−BPTI and its variants.

These results suggest a novel amide rotation hindrance mechanism regarding how the disulfide constraint leads to proteolysis resistance: The proteolysis of the cystine-knot peptide MCTI-A is retarded due to the higher free energy cost for the inevitable rotation of scissile peptide bond in the acylation reaction, and covalent constraint provided by disulfide bonds is the key factor to hinder the rotation of the amide bond.

To further examine this novel hypothesis as well as to elucidate the role of disulfide bond, we carried out corresponding simulations to two mutants of MCTI-A: C3S/C20S and C16S/C27S. The two mutants have similar conformation and hydrogen-bond networks as the wild type, except for the newly formed H bond with the introduced serine, as illustrated in Figure S3 and Table S2. Their binding affinity is only a little weaker than the wild type by 0.6 ± 0.3 and 1.2 ± 0.2 kcal/mol, respectively, by thermodynamic integration. (For calculation details, see the Supporting Information.) In comparison with the wild type, both mutants demonstrated enhanced flexibility, as shown in Figure S4. Because Cys3-Cys20 is the closest disulfide bond to the scissile bond, which would be expected to provide the strongest conformation restraint, the C3S/C20S mutant should lead to the lower barrier than the C16S/C27S mutant. As expected, the results in Figure 4a and Table S3 indicate that C3S/C20S mutant and C16S/C27S mutants have almost the same free energy barrier (~16 kcal/mol) for the initial nucleophilic attack step as the wild-type MCTI-A and SUB, but they have different barriers for TS2*. The free energy barriers at TS2* are 25.3, 23.1, 21.5, and 16.9 kcal/mol for MCTI-A (three disulfide bonds), C16S/C27S mutant (two disulfide bonds, the removed disulfide bond is the farthest to the scissile bond), C3S/C20S mutant (two disulfide bonds, the removed disulfide bond is the closest to the scissile bond), and hexapeptide substrate (zero


DOI: 10.1021/acs.jpclett.6b00373
J. Phys. Chem. Lett. 2016, 7, 1138−1142

disulfide bond), respectively. From EI to TS2* state, the carbonyl carbon transforms from trigonal to tetrahedral, and correspondingly the $\omega$ angle changes from near-planar to ~140° for all inhibitors and substrate, as reported in Table 1, which further supports the amide rotation hindrance mechanism.

Our next task is to directly elucidate the relationship between the rotation of the amide bond (the $\omega$ angle) and the acylation reaction barrier. Here we have calculated free energy change of the scissile amide bond rotation (the $\omega$ angle) at the protease−peptide Michaelis complex state for all four peptides with both ab initio QM/MM molecular dynamics simulations and classical MD simulations with umbrella sampling. As shown in Figure 4b,c, for both simulations with difference theoretical treatment of the scissile amide bond rotation there is a nearly linear correlation between the free energies for amide bond rotation free energy change from the planar to 140° and free energy barriers for reaction. This directly indicates that conformational constraints coming from disulfide formation lead to the hindrance of the rotation of the amide bond, which is directly correlated to the higher acylation reaction barrier. Meanwhile, in Figure 4c, rotation free energy change is calculated with Amber11 molecular dynamic package[29] and amber99SB[30,31] force fields, which is quite straightforward to be carried out and can be used as a parameter to predict the hydrolysis rate for MCTI-A-like inhibitors easily.

To examine whether this finding can be applied to other cystine-knot inhibitors, we calculated the rotation free energy changes of $\omega$ angle of BPTI using classical MD simulations and compared the results with the corresponding experimental free energy barrier[6] derived from transition-state theory,[32] as shown in Figure 4d. Our calculations show that there is also a strong correlation between the rotation energy change and experimental free energy barrier for the hydrolysis reaction, as shown in Figure 4d. This suggests that amide rotation hindrance could be one useful feature to estimate peptide proteolysis stability of cystine-knot peptides.

In summary, our work has suggested an amide rotation hindrance mechanism regarding how disulfide constraint leads to proteolysis resistance in cystine-knot peptides: The rotation of the scissile amide bond is hindered due to conformation constraint from the disulfide bonds, which leads to the higher free energy cost during the rotation of scissile peptide bond that takes place at the tetrahedral intermediate of the acylation reaction. By revealing a nearly linear correlation between free energy barriers of the peptide hydrolysis reaction and the amide rotation free energy changes calculated at the protease−peptide Michaelis complex state, we suggest that amide rotation hindrance could be one useful feature to estimate peptide proteolysis stability. It should be noted that the peptide proteolytic resistance is more general and not only limited to the cysteine-knot peptides. For those proteolytic-resistant peptides and proteins that do not contain any Cys-Cys disulfide bonds, such as cyclic peptides[33] and EGLIN C,[34] their respective proteolytic resistance mechanisms remain to be elucidated.

## ■ ASSOCIATED CONTENT

### Supporting Information

The Supporting Information is available free of charge on the ACS Publications website at DOI: 10.1021/acs.jpclett.6b00373. Computational details. Figure S1. Illustration of reaction mechanism of acylation reaction for serine protease and reaction coordinate chosen at each step of acylation. Figure S2. The inter-molecular hydrogen bonding network between porcine $\beta$-trypsin and MCTI-A. Figure S3. The structures of C3S/C20S and C16S/C27S variants in cartoon model at EI state. Figure S4. Calculated temperature factors for backbone heavy atoms of inhibitors from the MD simulations of enzyme-inhibitor state by Amber program. Figure S5. Illustration of atom names at active site. Table S1. List of key geometric parameters for the reactant, transition states, intermediate, and acyl-enzyme of acylation reaction for trypsin−MCTI-A based on B3LYP/6-31+G* QM/MM MD simulations. Table S2. Distance between the heavy atoms of intermolecular hydrogen bonds at the reactant complexes for trypsin−SUB and trypsin−inhibitors from MD simulations. Table S3. Relative free energy values for the reactant, transition states, intermediate, and acyl-enzyme of acylation reaction for trypsin−inhibitors and trypsin−substrate based on B3LYP/6-31+G* QM/MM MD simulations. (PDF)

## ■ AUTHOR INFORMATION


### Corresponding Authors

*Y. Zhou: E-mail: zhouyz@nju.edu.cn.

*Y. Zhang: E-mail: yingkai.zhang@nyu.edu.


### Notes

The authors declare no competing financial interest.

## ■ ACKNOWLEDGMENTS

This work was supported by the National Natural Science Foundation of China (Grant No. 21203090 to Y.Z.) and by the U.S. National Institutes of Health (R01-GM079223 to Y.Z.). We thank the High-Performance Computing Center of Nanjing University and NYU-ITS for providing computational resources.

## ■ REFERENCES


(1) Gongora-Benitez, M.; Tulla-Puche, J.; Albericio, F. Multifaceted Roles of Disulfide Bonds. Peptides as Therapeutics. *Chem. Rev.* **2014**, *114*, 901−926.

(2) Daly, N. L.; Craik, D. J. Bioactive Cystine Knot Proteins. *Curr. Opin. Chem. Biol.* **2011**, *15*, 362−368.

(3) Ackerman, S. E.; Currier, N. V.; Bergen, J. M.; Cochran, J. R. Cystine-Knot Peptides: Emerging Tools for Cancer Imaging and Therapy. *Expert Rev. Proteomics* **2014**, *11*, 561−572.

(4) Getz, J. A.; Rice, J. J.; Daugherty, P. S. Protease-Resistant Peptide Ligands from a Knottin Scaffold Library. *ACS Chem. Biol.* **2011**, *6*, 837−844.

(5) Kim, J. W.; Cochran, F. V.; Cochran, J. R. A Chemically Cross-Linked Knottin Dimer Binds Integrins with Picomolar Affinity and Inhibits Tumor Cell Migration and Proliferation. *J. Am. Chem. Soc.* **2015**, *137*, 6−9.

(6) Zakharova, E.; Horvath, M. P.; Goldenberg, D. P. Functional and Structural Roles of the Cys14-Cys38 Disulfide of Bovine Pancreatic Trypsin Inhibitor. *J. Mol. Biol.* **2008**, *382*, 998−1013.

(7) Hanson, W. M.; Domek, G. J.; Horvath, M. P.; Goldenberg, D. P. Rigidification of a Flexible Protease Inhibitor Variant Upon Binding to Trypsin. *J. Mol. Biol.* **2007**, *366*, 230−243.

(8) Huang, Q. C.; Liu, S. P.; Tang, Y. Q. Refined 1.6-Angstrom Resolution Crystal-Structure of the Complex Formed between Porcine Beta-Trypsin and Mcti-a, a Trypsin-Inhibitor of the Squash Family -




DOI: 10.1021/acs.jpclett.6b00373
J. Phys. Chem. Lett. 2016, 7, 1138−1142

Detailed Comparison with Bovine Beta-Trypsin and Its Complex. *J. Mol. Biol.* **1993**, *229*, 1022−1036.
(9) Ersmark, K.; Del Valle, J. R.; Hanessian, S. Chemistry and Biology of the Aeruginosin Family of Serine Protease Inhibitors. *Angew. Chem., Int. Ed.* **2008**, *47*, 1202−1223.
(10) Page, M. J.; Di Cera, E. Serine Peptidases: Classification, Structure and Function. *Cell. Mol. Life Sci.* **2008**, *65*, 1220−1236.
(11) Laskowski, M.; Qasim, M. A. What Can the Structures of Enzyme-Inhibitor Complexes Tell Us About the Structures of Enzyme Substrate Complexes? *Biochim. Biophys. Acta, Protein Struct. Mol. Enzymol.* **2000**, *1477*, 324−337.
(12) Laskowski, M.; Kato, I. Protein Inhibitors of Proteinases. *Annu. Rev. Biochem.* **1980**, *49*, 593−626.
(13) Otlewski, J.; Jelen, F.; Zakrzewska, M.; Oleksy, A. The Many Faces of Protease-Protein Inhibitor Interaction. *EMBO J.* **2005**, *24*, 1303−1310.
(14) Radisky, E. S.; King, D. S.; Kwan, G.; Koshland, D. E. The Role of the Protein Core in the Inhibitory Power of the Classic Serine Protease Inhibitor, Chymotrypsin Inhibitor 2. *Biochemistry* **2003**, *42*, 6484−6492.
(15) Radisky, E. S.; Koshland, D. E. A Clogged Gutter Mechanism for Protease Inhibitors. *Proc. Natl. Acad. Sci. U. S. A.* **2002**, *99*, 10316−10321.
(16) Radisky, E. S.; Lu, C. J. K.; Kwan, G.; Koshland, D. E. Role of the Intramolecular Hydrogen Bond Network in the Inhibitory Power of Chymotrypsin Inhibitor 2. *Biochemistry* **2005**, *44*, 6823−6830.
(17) Meier, K.; Choutko, A.; Dolenc, J.; Eichenberger, A. P.; Riniker, S.; van Gunsteren, W. F. Multi-Resolution Simulation of Biomolecular Systems: A Review of Methodological Issues. *Angew. Chem., Int. Ed.* **2013**, *52*, 2820−2834.
(18) Senn, H. M.; Thiel, W. Qm/Mm Methods for Biomolecular Systems. *Angew. Chem., Int. Ed.* **2009**, *48*, 1198−1229.
(19) Roux, B. The Calculation of the Potential of Mean Force Using Computer-Simulations. *Comput. Phys. Commun.* **1995**, *91*, 275−282.
(20) Boczko, E. M.; Brooks, C. L. Constant-Temperature Free Energy Surfaces for Physical and Chemical Processes. *J. Phys. Chem.* **1993**, *97*, 4509−4513.
(21) Zhou, Y.; Zhang, Y. Serine Protease Acylation Proceeds with a Subtle Re-Orientation of the Histidine Ring at the Tetrahedral Intermediate. *Chem. Commun.* **2011**, *47*, 1577−1579.
(22) Zhang, Y. K. Pseudobond Ab Initio Qm/Mm Approach and Its Applications to Enzyme Reactions. *Theor. Chem. Acc.* **2006**, *116*, 43−50.
(23) Zhang, Y. K.; Lee, T. S.; Yang, W. T. A Pseudobond Approach to Combining Quantum Mechanical and Molecular Mechanical Methods. *J. Chem. Phys.* **1999**, *110*, 46−54.
(24) Zhang, Y. K. Improved Pseudobonds for Combined Ab Initio Quantum Mechanical/Molecular Mechanical Methods. *J. Chem. Phys.* **2005**, *122*, 024114.
(25) Ishida, T.; Kato, S. Role of Asp102 in the Catalytic Relay System of Serine Proteases: A Theoretical Study. *J. Am. Chem. Soc.* **2004**, *126*, 7111−7118.
(26) Ishida, T.; Kato, S. Theoretical Perspectives on the Reaction Mechanism of Serine Proteases: The Reaction Free Energy Profiles of the Acylation Process. *J. Am. Chem. Soc.* **2003**, *125*, 12035−12048.
(27) Coombs, G. S.; Rao, M. S.; Olson, A. J.; Dawson, P. E.; Madison, E. L. Revisiting Catalysis by Chymotrypsin Family Serine Proteases Using Peptide Substrates and Inhibitors with Unnatural Main Chains. *J. Biol. Chem.* **1999**, *274*, 24074−24079.
(28) Martin, P. D.; Malkowski, M. G.; DiMaio, J.; Konishi, Y.; Ni, F.; Edwards, B. F. P. Bovine Thrombin Complexed with an Uncleavable Analog of Residues 7−19 of Fibrinogen a Alpha: Geometry of the Catalytic Triad and Interactions of the P1′, P2′, and P3′ Substrate Residues. *Biochemistry* **1996**, *35*, 13030−13039.
(29) Case, D. A.; Darden, T. A.; Cheatham, T. E., III; Simmerling, C. L.; Wang, J.; Duke, R. E.; Luo, R.; Walker, R. C.; Zhang, W.; Merz, K. M., et al. *Amber 11*; University of California: San Francisco, 2010.
(30) Cornell, W. D.; Cieplak, P.; Bayly, C. I.; Gould, I. R.; Merz, K. M.; Ferguson, D. M.; Spellmeyer, D. C.; Fox, T.; Caldwell, J. W.; Kollman, P. A. A 2nd Generation Force-Field for the Simulation of Proteins, Nucleic-Acids, and Organic-Molecules. *J. Am. Chem. Soc.* **1995**, *117*, 5179−5197.
(31) Hornak, V.; Abel, R.; Okur, A.; Strockbine, B.; Roitberg, A.; Simmerling, C. Comparison of Multiple Amber Force Fields and Development of Improved Protein Backbone Parameters. *Proteins: Struct., Funct., Genet.* **2006**, *65*, 712−725.
(32) Truhlar, D. G.; Garrett, B. C.; Klippenstein, S. J. Current Status of Transition-State Theory. *J. Phys. Chem.* **1996**, *100*, 12771−12800.
(33) Tyndall, J. D. A.; Fairlie, D. P. Macrocycles Mimic the Extended Peptide Conformation Recognized by Aspartic, Serine, Cysteine and Metallo Proteases. *Curr. Med. Chem.* **2001**, *8*, 893−907.
(34) Clark, E. A.; Walker, N.; Ford, D. C.; Cooper, I. A.; Oyston, P. C. F.; Acharya, K. R. Molecular Recognition of Chymotrypsin by the Serine Protease Inhibitor Ecotin from Yersinia Pestis. *J. Biol. Chem.* **2011**, *286*, 24015−24022.


DOI: 10.1021/acs.jpclett.6b00373
*J. Phys. Chem. Lett.* 2016, 7, 1138−1142